

# BIM-DEMATEL-BASED CAUSAL NETWORK MODEL FOR ACCURACY CONTROL IN MEP QUANTITY TAKEOFF

Di Wu<sup>1</sup>, Hongjie Zhang<sup>2\*</sup>

<sup>1</sup>The Architectural Engineering College of Anhui University of Applied Technology, Hefei, 230011, China

<sup>2</sup>MCC Communication Construction Group Co., Ltd., Beijing, 100081, China

**Abstract** - Mechanical and electrical installation directly influences project cost, schedule, and final quality. However, existing control methods mainly rely on manual experience and low-efficiency tools, which often lack precision and reliability. Therefore, this article innovatively proposes a causal network model that integrates building information modeling with decision testing and evaluation laboratories to improve the accuracy of mechanical and electrical engineering quantity calculations. This model enhances the recognition ability of nonlinear relationships between factors by introducing particle swarm optimization algorithm, and combines deep reinforcement learning to achieve adaptive adjustment of dynamic weights, thus constructing a high-precision visual causal structure. Test results on the SLABIM dataset show that the model achieves an accuracy of 99.12%, a recall of 99.54%, and an F1 score of 97.86%, which significantly outperform other comparative models. In convergence testing, the model reaches a convergence value of 0.06, which is 0.10 lower than the highest result among other models, and shows faster convergence speed overall. These outcomes demonstrate the model's accuracy and applicability in quantity takeoff control. The proposed model not only effectively improves the accuracy of calculations, but also presents causal paths clearly through visual networks, which helps to promote the development of intelligent and scientific management of mechanical and electrical engineering quantity accuracy.

**Keywords:** Causal network; BIM-Dematel; Quantity takeoff accuracy; Particle swarm optimization; Mechanical and electrical installation; Particle Swarm Optimization; Deep Reinforcement Learning.

## 1. Introduction

With the expansion of urban development, mechanical and electrical installation has become increasingly common in construction operations. mechanical and electrical installation work plays a direct role in determining project progress and overall quality [1]. As the foundation of project success, quantity takeoff accuracy management is vital. Errors in quantity takeoff can reduce project benefits and increase risks, while high-quality control ensures successful project delivery [2]. Traditional control methods for MEP quantity takeoff primarily rely on manual judgment, two-dimensional drawings, and sample-based statistics [3]. These methods suffer from limited accuracy, poor information coordination, and low efficiency. As a result, improving the efficiency of mechanical and electrical installation quantity takeoff accuracy management has become a key research focus [4]. With advances in computing technology, data-driven control models are revealing

new possibilities. In particular, the combination of Building Information Modeling (BIM) and Decision-making Trial and Evaluation Laboratory (Dematel) forms a BIM-Dematel causal network. This approach enables accurate identification of core driving factors, full-process control driven by data, and visualized multi-factor relationship analysis [5]. Applying this network to MEP quantity takeoff accuracy management helps clearly identify key influencing factors and quantify their logical relationships, thereby improving control efficiency. This paper introduces an innovative BIM-Dematel-based causal network for managing mechanical and electrical installation quantity takeoff accuracy. The goal is to build a dynamic and visualized factor network that allows for prioritized control and informed decision-making. The proposed method highlights interdisciplinary integration and a shift from static evaluation to dynamic management, contributing to both business and engineering management practices.

## 2. Related Works

BIM has several advantages, such as generating three-dimensional spatial diagrams, automating parameter models, and supporting continuous analysis of events. It has played an important role in various fields, including construction, infrastructure, and urban planning. Scholars from around the world have studied its applications. To expand BIM capabilities for solving construction problems, Saad A et al. put forward a method to upgrade BIM plug-ins. They analyzed 34 different plug-ins using a systematic evaluation approach and found that customized plug-ins performed better. Based on common features extracted from plug-in systems, they proposed a framework for dynamic programming of BIM plug-ins [6]. To address the slow adoption of BIM in the construction industry, Umar T and his team developed a BIM acceleration process. This approach reduced repetitive work by using parametric modeling, generated real-time shared data on a common platform, and automatically created construction simulations and scheduling plans according to user requirements [7]. Zhou D et al. proposed the use of BIM, geographic information systems, and the Internet of Things to accurately identify key nodes in road construction, addressing the difficulty of controlling the accuracy of cofferdam lowering. BIM models were used to guide construction, improving on-site work efficiency and ensuring comprehensive control and safety management [8]. Automatic quantity estimation based on high-quality BIM models can not only significantly improve the efficiency of engineering quantity extraction, but also ensure the accuracy and consistency of results by avoiding manual intervention, thereby providing reliable basis for project cost control. To this end, Chen Z et al. investigated the role of BIM in simplifying the life cycle assessment process to improve efficiency and accuracy, explored the performance and limitations of various BIM software and life cycle assessment (LCA) tools, and introduced the characteristics of BIM and LCA integration cases [9]. Zheng B et al. used quantitative techniques to evaluate the accuracy and efficiency of four typical BIM and LCA integrated solutions, and found that traditional methods can achieve the highest accuracy in engineering quantity calculation, while parametric modeling methods are superior to industry based methods in terms of engineering quantity calculation efficiency [10].

On the other hand, the Dematel method helps visualize causal relationships. It requires neither large historical datasets nor heavy reliance on expert knowledge, making it suitable for analyzing complex problems in engineering systems and social sciences.

In a study on evaluating alternative banking systems, Banerjee T et al. developed a model combining T-spherical fuzzy decision-making and Dematel. They used triangular fuzzy numbers to quantify expert opinions, built and calculated a direct impact matrix, and identified key dimensions by determining the importance and causal relationships of evaluation criteria [11]. Murugan M and his team proposed a fuzzy Dematel algorithm to explore obstacles in electric vehicle adoption. They collected expert input and user data, then used Dematel to analyze causal relationships and impact degrees. Fuzzy logic was applied to handle data uncertainty, and a relative importance coefficient helped prioritize user concerns [12].

Quantity takeoff accuracy management often serves as a stabilizer for project development. High accuracy leads to positive project cycles, while low accuracy can cause systemic errors. Researchers have studied this topic from different perspectives. To improve facial recognition accuracy on mobile devices, Opanasenko V M et al. proposed a method combining recognition operators with decision rules. This structure estimated proximity between test samples and categories, classified results based on decision rules, and optimized parameters using a set of linear polynomial operators [13]. To improve the performance of hydraulic-free piston engines, Bing Y U et al. developed a dual-iteration optimization algorithm. They built a simulation model and iteratively optimized parameters through inner and outer loops to improve performance and reach optimal convergence [14]. To improve anti-interference performance in weak magnetic field control of aircraft motors, Wang Y et al. proposed a deep reinforcement learning algorithm. This method created a disturbance-rejection controller, optimized sensitivity parameters, and quickly converged to improve control performance [15].

In summary, the combination of BIM and Dematel forms a BIM-Dematel causal network that integrates the spatial data advantages of BIM with the causal analysis strength of Dematel. This structure significantly improves the efficiency and accuracy of analyzing complex problems in target events. However, many current systems still face challenges such as unmanageable data complexity and poor coordination efficiency, which limit the effectiveness of quantity takeoff accuracy management. Therefore, this study integrates the BIM-Dematel causal network into mechanical and electrical installation quantity takeoff accuracy control, aiming to enhance decision-making precision and data analysis speed for complex systems, and to provide technical support for mechanical and electrical installation processes.

### 3. The BIM-Dematel Causal Network Control Model for Quantity Takeoff Accuracy

#### 3.1 Optimization of the BIM-Dematel Causal Network based on Particle Swarm Optimization

To ensure the accuracy of cost estimation, managers use systematic methods to reduce errors in quantity calculation. This supports the purpose of quantity takeoff accuracy control, which plays a key role in reducing risks and improving efficiency [16]. According to the Dematel network, the relationships among influencing factors help identify key elements

that affect quantity takeoff accuracy. The method provides advantages in locating key factors and performing dynamic optimization. BIM features three-dimensional digital characteristics that help reduce calculation errors and offer high accuracy and efficiency. However, existing methods that combine BIM with Dematel mainly remain at the level of static causal analysis, making it difficult to capture complex nonlinear relationships and respond to dynamic changes in a timely manner.

The integration of both methods offers advantages for managing quantity takeoff accuracy in mechanical and electrical installation. Therefore, this study introduces the BIM-Dematel causal network. The process of this network is shown in Figure 1.

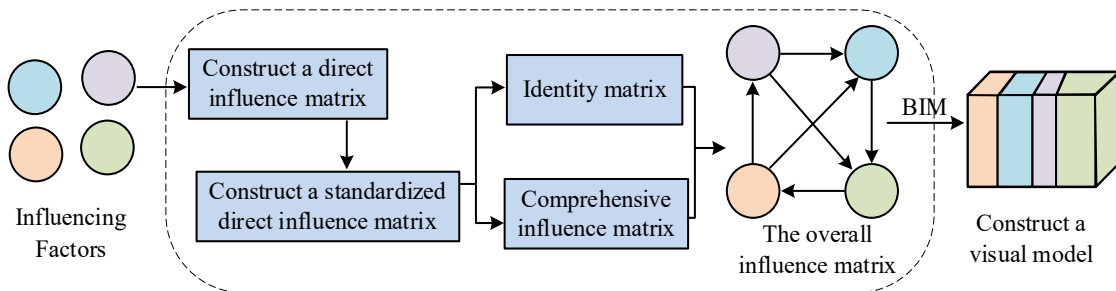


Figure 1: Operation flow chart of BIM-Dematel causal network

As shown in Figure 1, the BIM-Dematel causal network identifies the key influencing factors of a target. It builds a direct impact matrix based on the influence intensity among factors. After normalization, a standardized direct impact matrix is formed. Then, using the identity matrix and the total impact matrix, the complete impact matrix is generated and imported into the BIM program to produce a visualized model. The direct impact matrix is constructed based on expert scoring, as shown in Equation (1).

$$X = \begin{bmatrix} 0 & x_{12} & \cdots & x_{1n} \\ x_{21} & 0 & \cdots & x_{2n} \\ \vdots & \vdots & \ddots & \vdots \\ x_{n1} & x_{n2} & \cdots & 0 \end{bmatrix} = (x_{ij})_{n \times n} \quad (1)$$

In Equation (1),  $n$  represents the number of influencing factors.  $x_{ij}$  indicates the degree to which factor  $i$  directly affects factor  $j$ . Both  $i$  and  $j$  are integers ( $1 \leq i \leq n, 1 \leq j \leq n$ ). If  $i = j$ , then  $x_{ij} = 0$ . The centrality  $m_i$  reflects the importance of the factor in the system. The causality  $n_i$  indicates the degree of causal relation with other factors. Their calculation equations are shown in Equation (2).

$$\begin{cases} m_i = f_i + e_i, (i = 1, 2, \dots, n) \\ n_i = f_i - e_i, (i = 1, 2, \dots, n) \end{cases} \quad (2)$$

In Equation (2),  $f_i$  represents the influence degree of factor  $i$ , and  $e_i$  represents the degree of being influenced. After determining each factor and the degree of relation, the complete impact matrix is constructed, as shown in Equation (3).

$$(A + E) \neq (A + E)^2 \neq \cdots \neq (A + E)^{k-1} = (A + E)^k = M \quad (3)$$

In Equation (3),  $A$  is the adjacency matrix,  $E$  is the identity matrix, and  $k$  is the influence power. After constructing the complete impact matrix, the matrix is divided multiple times to form a hierarchical structure. Arrows are used to connect related factors, producing a structural model of factor impacts. The BIM-Dematel causal network relies heavily on causal matrix analysis and struggles to capture indirect dependencies among multiple factors. This can lead to repeated or missing calculations. To address this limitation, this study introduces Particle Swarm Optimization (PSO). PSO enables individuals to iterate independently and adjust directions based on the best individual and global positions. It gradually approaches the optimal solution [17]. The optimization process of PSO is shown in Figure 2.

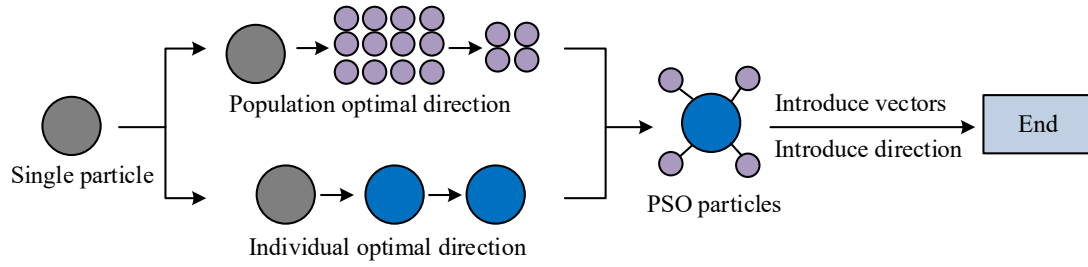


Figure 2: Flowchart of PSO algorithm particle optimization

As shown in Figure 2, the PSO algorithm randomly generates particle positions and calculates the fitness of each particle. Based on these values, it selects the best global or individual positions. New particles are introduced by adjusting vectors and directions to search for the optimal solution. The fitness of a particle is calculated using Equation (4).

$$MAE = \frac{1}{n} \sum_{i=1}^n |f(x) - y| \quad (4)$$

In Equation (4),  $n$  is the number of particles.  $f(x)$  is the fitness function.  $y$  represents the comfort value. After calculating the fitness of each particle, the particles continue the optimization process. Global optimization is shown in Equation (5).

$$v_{id}^{k+1} = wv_{id}^k + c_1r_1(pbest_{id}^k - x_{id}^k) + c_2r_2(pbest_d^k - x_{id}^k) + grad_{id}^k + grad_d^k \quad (5)$$

In Equation (5),  $w$  is the weight,  $v$  is the second-order moment estimate of the gradient,  $c$  represents the particle, and  $r$  is the particle radius.  $grad_{id}^k$  and  $grad_d^k$  indicate the direction gradients during the  $k$ -th iteration.  $pbest_{id}^k$  and  $pbest_d^k$  are the particle values after  $k$  iterations during network training. The search dimension is  $d$ . Individual optimization is expressed in Equation (6).

$$v_d^{k+1} = pbest_{id}^k \cdot w \cdot rand() \cdot grad_{id}^k \quad (6)$$

In Equation (6),  $rand(\cdot)$  is a distance value between 0 and 1 and is randomly assigned. Through iterative optimization, PSO generates new particles, which can reconnect nonlinear influences among factors. The BIM-Dematel causal network identifies influence relationships among factors and generates a visual graph, which improves accuracy in quantity takeoff. Therefore, this study integrates PSO and the BIM-Dematel causal network to form a PSO-BIM-Dematel causal network. The process is shown in Figure 3.

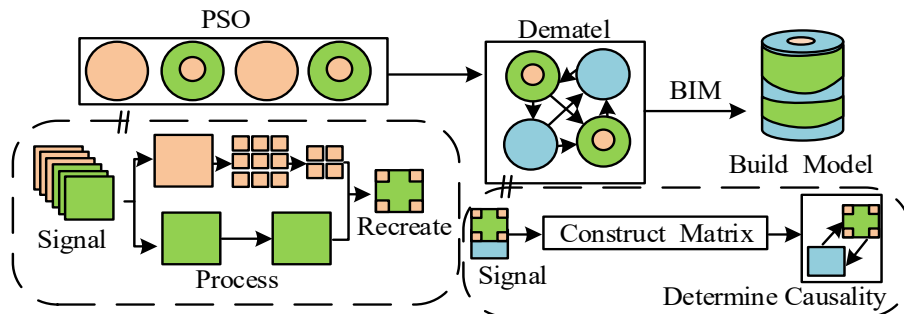


Figure 3: PSO-BIM-Dematel causal network flow chart

As shown in Figure 3, PSO is used as a pre-processing module to optimize particles into PSO particles. These then enter the BIM-Dematel module, where expert scoring creates the initial matrix. After normalization, a standardized matrix is obtained. The comprehensive impact matrix is then calculated, followed by the overall impact matrix. This final matrix is imported into the BIM program to generate a visualized interface, showing the network of influence relationships among factors. Unlike existing hybrid methods that simply stack BIM with Dematel, the fundamental difference of the proposed PSO-BIM-Dematel model lies in the innovative

introduction of PSO as a preprocessing module for the network, enabling the system to optimize and reveal complex nonlinear relationships between factors before constructing causal networks, thereby significantly enhancing the accuracy and structural rationality of subsequent causal analysis. The precision of PSO particle optimization is shown in Equation (7).

$$\theta = \theta - \eta \cdot \nabla_{\theta} J(\theta; x^{(i)}; y^{(i)}) \quad (7)$$

In Equation (7),  $\theta$  is the parameter to be optimized,  $J(\cdot)$  is the loss function, and  $\eta$  is the

learning rate. The normalization process of the initial matrix is shown in Equation (8).

$$\begin{cases} r_i = \sum_{j=1}^n x_{ij} \\ c_j = \sum_{i=1}^n x_{ij} \end{cases} \quad (8)$$

$$T = \lim_{K \rightarrow \infty} (X + X^2 + \dots + X^K) = \lim_{K \rightarrow \infty} (E + X + X^2 + \dots + X^{K-1}) \quad (9)$$

In Equation (9),  $X$  is the direct impact matrix,  $E$  is the identity matrix, and  $K$  is the number of factors. When the BIM-Dematel causal network matches relationships among factors, PSO helps refine individual elements and reveals nonlinear connections among multiple factors. This compensates dependence on the causal matrix and improves the accuracy of quantity takeoff.

### 3.2 The Control Model for Quantity Takeoff Accuracy in Mechanical and Electrical Installation

Although the PSO-BIM-Dematel causal network supports quantity takeoff accuracy control in

In Equation (8),  $r_i$  is the sum of each row,  $c_j$  is the sum of each column, and  $n$  is the number of particles. The comprehensive impact matrix  $T$  represents the overall effect of both direct and indirect impacts among factors, as shown in Equation (9).

mechanical and electrical installation, dynamic events such as design changes often occur during the installation process.

The network struggles to capture real-time causal relationships among changing factors, which reduces accuracy [18]. Therefore, this study introduces deep reinforcement learning (DRL), which adjusts factor weights in the PSO-BIM-Dematel network through policy networks to enable adaptive learning and adjustment of dynamic relationships.

The DRL process framework is shown in Figure 4.

As shown in Figure 4, the DRL algorithm initializes the environment.

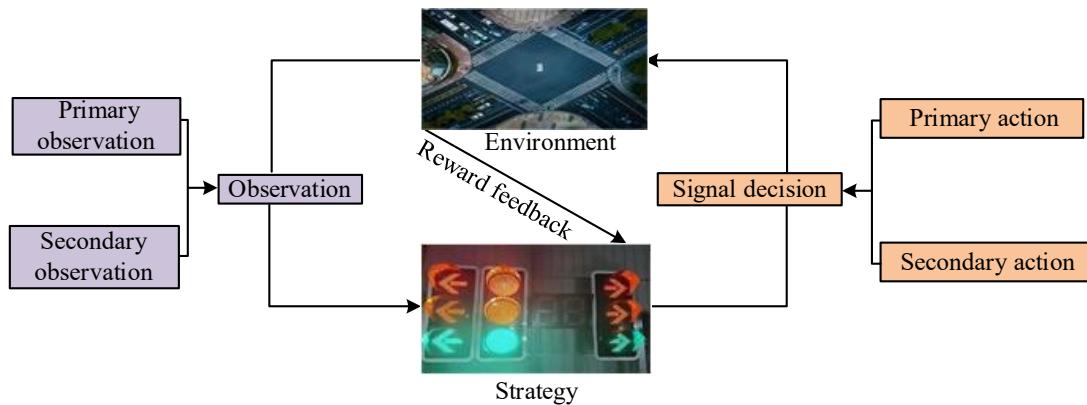


Figure 4: DRL framework diagram (Image source from: <https://freeicons.io/iconset/free-icons-set>)

Before a signal decision occurs, the agent makes primary and secondary observations based on the environment. The signal decision is passed to the action decision, which then changes the environment. During action execution, the agent receives a feedback reward, which is sent back to the signal decision and used to update the signal state. The optimal policy decision  $a$  is obtained as shown in Equation (10).

$$a = \begin{cases} \text{are max } Q(s, a) & \text{with probability } 1 - \varepsilon \\ \text{random action} & \text{with probability } \varepsilon \end{cases} \quad (10)$$

In Equation (10),  $Q$  represents the action corresponding to the maximum value, and  $\varepsilon$  represents the probability of exploration. The agent uses the feedback reward to perform iterative calculations and obtain the maximum action value  $P$ , as shown in Equation (11).

$$P(s, a) = P(s, a) + \alpha(r + \gamma \max_{a'} P(s', a') - P(s, a)) \quad (11)$$

In Equation (11),  $\alpha$  is the learning rate,  $\gamma$  is the discount factor,  $P(s, a)$  is the maximum value of action  $a$  executed by  $s$  in the current state, and  $P(s', a')$  is the maximum value when action  $a'$  leads to state  $s'$ . Different maximum values correspond to different learning rates, as shown in Equation (12).

$$L_{t,i} = \nabla_{\theta_i} J(\theta_{t,i}) \quad (12)$$

In Equation (12),  $L_{t,i}$  is the gradient,  $\theta_i$  is the optimized parameter, and  $J$  is the optimization coefficient. DRL has strong representational capacity and dynamic decision-making capabilities. It performs well in dynamic environments and spatial modeling. However, it still shows weaknesses in



continuous space modeling and large-scale data processing [19]. To address these limitations, this study introduces the Deep Q-Network (DQN). DQN

approximates the Q-value function through deep neural networks, improving DRL's performance in those areas. The DQN process is shown in Figure 5.

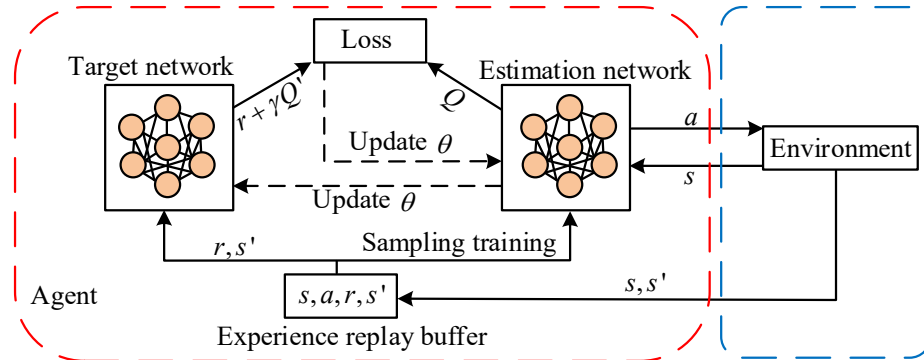


Figure 5: Schematic diagram of DQN framework

As shown in Figure 5,  $s$  is the gradient state,  $s'$  is the gradient state under the target state,  $a$  is the policy action,  $Q$  is the target network,  $\theta$  is the network coefficient,  $\gamma$  is the discount factor, and  $r$  is the gradient distance. DQN introduces experience replay and a target network. Experience replay stores interactions between the agent and the environment in a buffer. Once enough data accumulates in the buffer, random samples are drawn for training, improving stability. The target network updates its weights periodically, which reduces the risk of local non-convergence. The online network minimizes the loss function to approximate the target network, as shown in Equation (13).

$$L(\lambda) = Z[(r_t + \gamma \max_a Q(s_{t+1}, a_{t+1}, \lambda') - Q(s_t, a_t, \lambda))^2] \quad (13)$$

In Equation (13),  $\lambda$  is the parameter of the online  $Q$  network,  $\lambda'$  is the parameter of the target  $Q$  network, and  $Z$  is the stored value. This method determines the policy without requiring large datasets and improves algorithm efficiency, as shown in Equation (14).

$$\nabla_{\theta} Z(\pi_{\theta}) = \int_s \rho^{\pi}(s) \int_A \nabla_{\theta} \pi_{\theta}(a|s) Q^{\pi}(s, a) da ds \quad (14)$$

In Equation (14),  $\rho^{\pi}$  follows a distribution,  $\pi_{\theta}$  follows a second-order distribution, and  $Q^{\pi}(s, a)$  is the mathematical expectation. The action is executed as shown in Equation (15).

$$a_t = \arg \max_a Q(s_t, a; \theta) \quad (15)$$

In Equation (15),  $\arg$  is the greedy strategy, and  $s_t$  is the updated state. After data recognition, DQN first initializes the network structure and builds the experience pool. The agent interacts with the environment and sends the termination signal to the buffer. It then randomly samples from the buffer to compute the target  $Q$  value and iterates until convergence [20]. DQN compensates for DRL's weaknesses in handling continuous space modeling and large-scale data. When combined with the PSO-BIM-Dematel causal network, it enhances quantity takeoff accuracy in mechanical and electrical installation. Therefore, this study proposes the DQN-DRL-PSO-BIM-Dematel causal network. The integrated process is shown in Figure 6.

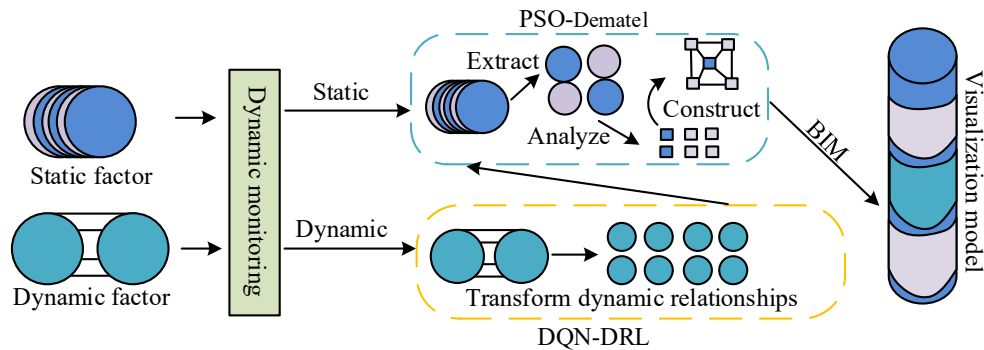


Figure 6: The structure of the proposed fusion network

As shown in Figure 6, the DQN-DRL-PSO-BIM-Dematel causal network integrates DQN and DRL for intelligent

decision-making by learning optimal strategies through trial and error. PSO optimizes model parameters and improves search efficiency. BIM

provides multidimensional data and spatial information to analyze causal relationships among factors. In the integrated process, DRL and DQN perform strategy learning based on data, PSO handles factor optimization, and Dematel identifies causal relationships among factors to build a causal network. BIM then generates a visual model. In summary, the DQN-DRL-PSO-BIM-Dematel causal network not only mitigates challenges related to continuous space modeling and the curse of dimensionality but also improves computational efficiency and accuracy through DRL, resulting in a visualized model to support quantity takeoff accuracy control in mechanical and electrical installation.

#### 4. Performance Analysis of Precision Control Model for Mechanical and Electrical Installation Calculation

##### 4.1 The effectiveness of Engineering Calculation Accuracy Control using PSO-BIM-Dematel Causal Network

To verify the advantages of the PSO-BIM-Dematel causal network, this study compared it with the Analytic Network Process-Building Information Modeling-Decision-making Trial and Evaluation Laboratory (ANP-BIM-Dematel), the Building

Information Modeling-Matrixed Impacts Croises-Multiplication Appliance Classique (BIM-MICMAC), and the Geographic Information System-Structural Equation Modeling (GIS-SEM) through training and testing.

The experiments were conducted using high-performance equipment. The system version was Windows 10, the operating system was Ubuntu 20.04, the deep learning framework was PyTorch, the optimizer was Adam, the programming language was Python 4.26.06, the BIM modeling tool was Autodesk Revit, the visualization tool was Gephi, the GPU was NVIDIA RTX 4090, the CPU was Intel i7, and the memory was 128 GB. To ensure the authenticity and reliability of the results, the SLABIM and Datarade datasets were used for training and testing. To verify the impact of parameter changes on the PSO-BIM Dematel causal network, this study conducted a systematic sensitivity analysis of its key parameters, including particle count, iteration times, and learning rate.

The experiment used the method of controlling variables to test the precision, recall, and F1 score of the model under different parameter combinations on the SLABIM dataset. The results of parameter sensitivity analysis are shown in Table 1.

Table 1. Parameter sensitivity analysis results

Particle count	Iteration count	Learning rate	Precision	Recall	F1-Score
50	300	0.01	0.979	0.983	0.981
100	300	0.01	0.982	0.986	0.984
150	300	0.01	0.982	0.986	0.984
100	500	0.01	0.986	0.989	0.988
100	700	0.01	0.985	0.988	0.987
100	500	0.005	0.982	0.987	0.985
100	500	0.02	0.983	0.987	0.986

From Table 1, it can be seen that increasing the number of particles from 50 to 100 can lead to improvements in three indicators while keeping other parameters constant. But as the number of particles continued to increase to 150, there was no further improvement in performance, indicating that a particle count of 100 was sufficient. When the number of iterations increased from 300 to 500, there was a significant improvement in performance (F1 score increased from 0.984 to 0.988), and when it continued to increase to 700, there was no further improvement, indicating that performance had reached saturation. A learning rate of 0.01 can

achieve optimal performance, while a learning rate that is too low (0.005) or too high (0.02) can cause a slight decrease in model performance. Overall analysis shows that the model performs best when the number of particles is 100, the number of iterations is 500, and the learning rate is 0.01. Therefore, the study will set the number of particles to 100, the number of iterations to 500, the learning rate to 0.01, the inertia weight to 0.8, and both individual and social learning factors to 1.5. To verify the accuracy of the PSO-BIM-Dematel causal network, this study tested the average loss values using the SLABIM dataset. The results are shown in Figure 7.

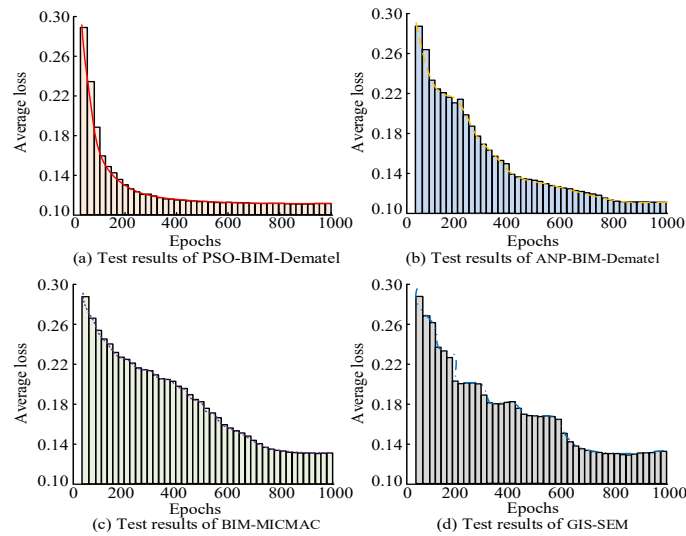


Figure 7: Average loss value training and testing results

As shown in Figure 7(a), the PSO-BIM-Dematel causal network reached an average loss value of 0.12 at 280 iterations and then stabilized. In the application scenario of precision control of mechanical and electrical installation calculation, the calculation of engineering quantity usually involves a large amount of component information and complex system relationships, and the calculation process is time-consuming and prone to errors. The fast convergence feature of PSO-BIM Dematel network can efficiently process complex computational data and quickly capture indirect dependencies between various factors, which helps to provide more accurate analysis for the computational complexity of mechanical and electrical installation. As shown in Figure 7(b), the ANP-BIM-Dematel network stabilized at an average loss value of 0.13, but it required 800 iterations, which was significantly more than the PSO-BIM-Dematel causal network. As shown in

Figures 7(c) and 7(d), both the BIM-MICMAC and GIS-SEM networks had higher average loss values, and the GIS-SEM network exhibited large fluctuations during testing. The results indicate that the PSO BIM Dematel causal network has a lower final loss value, indicating that the network has established a more accurate input-output mapping relationship. This provides a fundamental guarantee for achieving low errors in subsequent engineering quantity calculations, effectively supporting project cost control and schedule management. In order to ensure the accuracy of automated calculation from the source, this study evaluated the performance of various models in identifying the characteristics of mechanical and electrical installation calculation, which is a prerequisite for achieving high-precision automated calculation. This study focuses on three indicators: accuracy, recall rate, and F1 score. The results are shown in Figure 8.

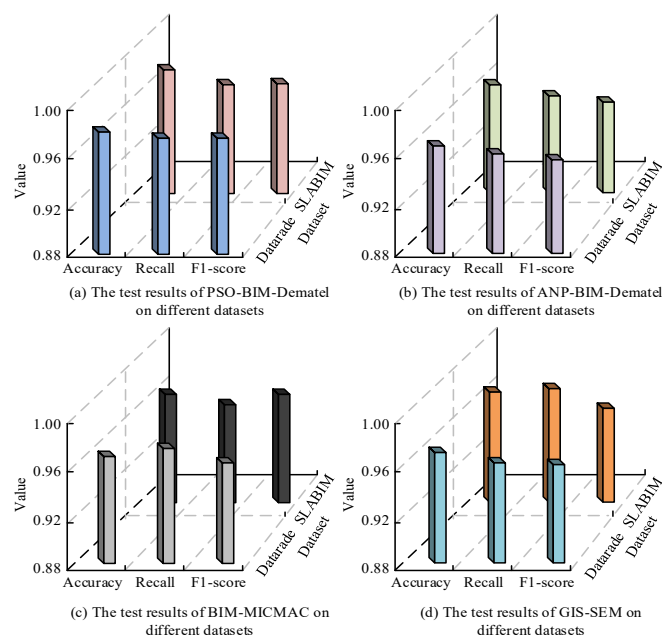


Figure 8: Comparison of the recognition performance of computational features in mechanical and electrical installation among various models



As shown in Figure 8, in the SLABIM dataset, the PSO-BIM-DemateI causal network achieved a precision of 0.98, which was 0.02 higher than the lowest score from the ANP-BIM-DemateI network (0.94). This advantage means that in the process of identifying computational features in mechanical and electrical installation, the PSO-BIM Demater network can more accurately filter out effective features related to computational complexity, effectively avoiding misjudging structural components or other system components as mechanical and electrical components. Its recall was 0.97, which was 0.03 higher than the lowest score from the GIS-SEM network (0.94). The high recall rate indicates that in actual electromechanical installation engineering, the PSO-BIM Demater network can comprehensively identify most of the features related to the computational complexity of electromechanical installation, minimizing the risk of "missing" key components. Its F1-score reached 0.99, outperforming all other models. In the Datarade dataset, the PSO-BIM-DemateI network achieved a

precision of 0.99, a recall of 0.98, and an F1-score of 0.99, again higher than all comparison models. The results indicate that the PSO-BIM DemateI causal network can accurately and comprehensively identify mechanical and electrical installation components from complex BIM models. The high-precision recognition capability provides high-quality and reliable data input for subsequent automated engineering quantity calculation, directly eliminating the calculation deviation caused by component misidentification from the source, and laying a solid data foundation for project cost control.

To directly verify the effectiveness of the proposed model in the core tasks of mechanical and electrical installation, this study evaluated the errors of each model in calculating three key mechanical and electrical engineering quantities: duct area, pipe length, and cable tray quantity. The experiment used the most representative mean absolute percentage error (MAPE) in the field of engineering cost as the core performance indicator, and the results are shown in Table 2.

Table 2. Comparison of MAPE of Various Models in the Calculation of Mechanical and Electrical Installation Engineering Quantity

Models	Air duct area	Pipe length	Number of cable trays
GIS-SEM	7.22%	5.50%	7.55%
BIM-MICMAC	5.78%	6.14%	6.84%
ANP-BIM-DemateI	4.51%	3.93%	5.18%
PSO-BIM-DemateI	2.09%	1.81%	2.47%

From Table 2, it can be seen that the PSO-BIM-DemateI causal network achieved the lowest MAPE in all three categories of engineering quantity calculations, with a stable MAPE value controlled within 2.5%. This means that in engineering practice, the PSO-BIM-DemateI network can control the calculation deviation of material usage at an extremely low level, effectively avoiding the risk of material waste or shortage caused by calculation deviation. In contrast, the error rates of ANP-BIM Mattel and BIM-MICMAC models are relatively high, about 1.5 to 2 times higher than those of PSO models. The performance of the GIS-SEM model is the most unstable, especially in calculating the area of air ducts and the number of cable trays, where errors are the largest, making it difficult to meet the strict requirements for calculation accuracy in mechanical and electrical installation engineering.

The experimental results fully demonstrate that the proposed PSO-BIM-DemateI causal network can efficiently handle complex spatial and system relationships in BIM models, output highly accurate engineering quantity data, and is an effective solution

for achieving precision control of mechanical and electrical installation calculations.

#### 4.2 Evaluation of the Practicality of the PSO-BIM-DemateI Control Model

After verifying the performance of the PSO-BIM-DemateI causal network, this study further evaluated the accuracy control model for mechanical and electrical installation based on this network. The model was compared with those constructed using Building Information Modeling-Decision Making Trial and Evaluation Laboratory-Interpretative Structural Modeling Method (BIM-DemateI-LSM), Building Information Modeling-Technology Acceptance Model-TCP Offload Engine (BIM-TAM-TOE), and Building Information Modeling-Work Breakdown Structure-Risk Breakdown Structure (BIM-WBS-RBS). To ensure the reliability of the experimental results, Autodesk Revit 2022 was used as the BIM modeling software, Python 3.92.15 as the algorithm development platform, the Revit API as the BIM data interface, NVIDIA RTX 3080 as the GPU, Intel Core i7-11700K as the CPU, and 256 GB memory. The MagiCAD and Genome datasets were used for model

training and evaluation. To verify the feature recognition accuracy of the control model based on the PSO-BIM-Dematel causal network, the precision,

recall, and F1-score of the model were compared with those of the three other models. The training and testing results are shown in Figure 9.

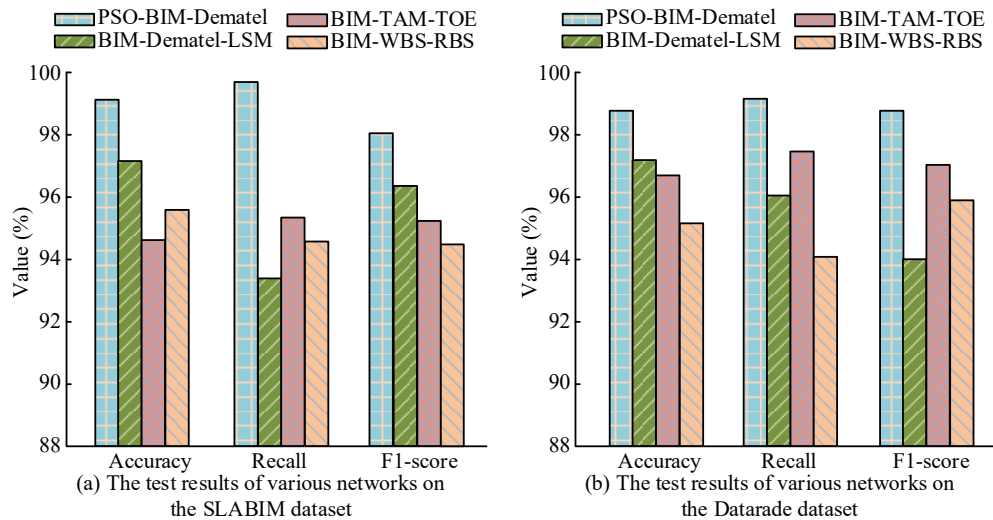


Figure 9: Precision, recall, and F1 score test results

As shown in Figure 9(a), in the SLABIM dataset, the PSO-BIM-Dematel model achieved a precision of 99.12%, which was 4.28% higher than the lowest result of 94.84% from the BIM-TAM-TOE model. Its recall was 99.54%, 6.28% higher than the lowest result of 93.26% from the BIM-Dematel-LSM model. Its F1-score was 97.86%, which outperformed all comparison models. As shown in Figure 9(b), in the Datarade dataset, the PSO-BIM-Dematel model achieved a precision of 98.56%, a recall of 99.51%,

and an F1-score of 98.23%, all higher than the other models. In summary, this model showed significant advantages in accuracy, completeness, and overall performance in feature recognition, confirming its generalization ability and reliability across different datasets. To further verify the convergence performance of the PSO-BIM-Dematel model, this study compared it with the other models using the SLABIM and Datarade datasets. The results are shown in Figure 10.

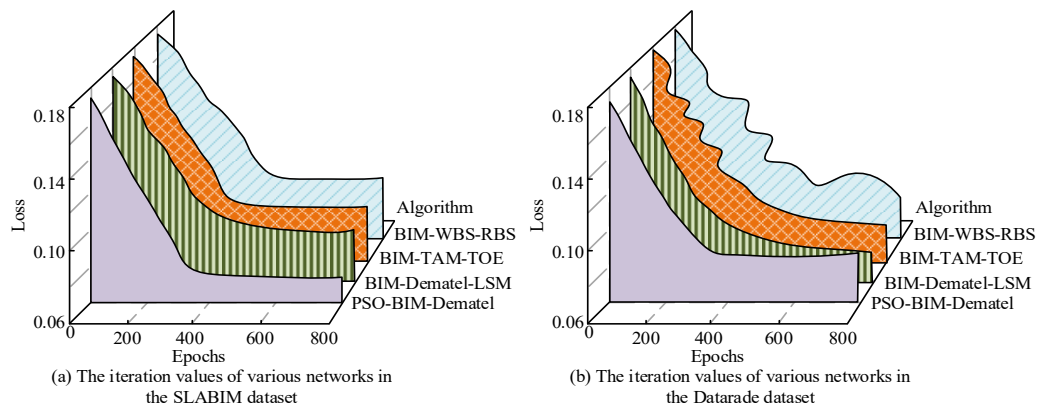


Figure 10: Convergence test results comparison

As shown in Figure 10(a), in the SLABIM dataset, the PSO-BIM-Dematel model reached a stable convergence value of 0.06 after 400 iterations, which was lower than that of the other models and required fewer iterations. As shown in Figure 10(b), in the Datarade dataset, the PSO-BIM-Dematel model also stabilized at a convergence value of 0.09 after 400 iterations. In contrast, the BIM-Dematel-LSM model reached a loss value of 0.12 when stabilized, while the BIM-TAM-TOE and BIM-WBS-RBS models showed

large fluctuations during testing, with loss values of 0.13 and 0.16, respectively, and required more iterations. In summary, the PSO-BIM-Dematel model maintained good convergence and faster convergence speed across different datasets.

To further demonstrate the model's accuracy, this study conducted a classification test of mechanical and electrical installation systems using the SLABIM dataset.

The results are shown in Figure 11.

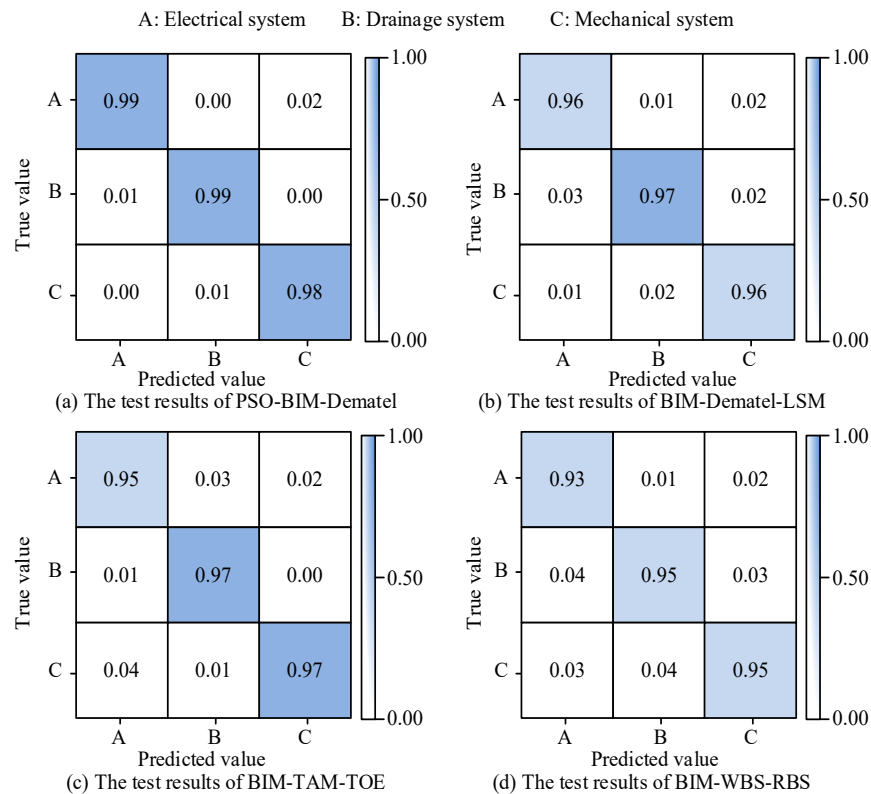


Figure 11: Results of the electromechanical installation classification identification test

As shown in Figure 11(a), the PSO-BIM-Dematel model performed well in system recognition. Its recognition accuracy for the electrical system reached 99%, with only 1% misclassified as drainage. The drainage system also reached 99% accuracy, which was 4% higher than the 95% result from the BIM-WBS-RBS model. The mechanical system was recognized with 98% accuracy, outperforming all comparison models. To further validate the effectiveness and generalization ability of the proposed PSO-BIM-Dematel model in real industrial environments, this study constructed a composite benchmark test set. This test set integrates representative electromechanical models from the SLABIM dataset and introduces a large-scale commercial complex MEP model extracted and anonymized from actual projects, covering major systems such as air ducts, water pipes, and cable

trays, with approximately 85000 component instances. The experiment adopts five fold cross validation, with F1 score, precision, and recall as the core evaluation indicators. Select Geographic Information System Structural Equation Modeling (GIS-SEM), Building Information Modeling Matrix Impact Multiplication Equipment Classic (BIM-MICMAC), and Analysis Network Process Building Information Modeling Decision Testing and Evaluation Laboratory (ANP-BIM Dematel) as baseline models. All models run under the same data partitioning and hardware environment. To evaluate the statistical significance of performance differences, paired t-tests were performed on the results of PSO-BIM-Dematel and each baseline model, with a significance level of  $\alpha=0.05$ . The statistical comparison results with the baseline model are shown in Table 3.

Table 3. Statistical comparison results with baseline model

Models	Precision	Recall	F1-Score
GIS-SEM	0.941±0.012*	0.931±0.016*	0.935±0.012*
BIM-MICMAC	0.957±0.010*	0.948±0.012*	0.951±0.009*
ANP-BIM-Dematel	0.971±0.008*	0.966±0.009*	0.968±0.007*
PSO-BIM-Dematel	0.985±0.004	0.988±0.003	0.987±0.003

Note: "\*" indicates a significant difference compared to PSO-BIM-Dematel,  $P<0.01$ .

From Table 3, it can be seen that the proposed PSO-BIM-Dematel model still demonstrates good performance on the composite industrial benchmark test set, with the highest average F1 score, precision, and recall rate of 0.987, 0.985, and 0.988, respectively,

significantly higher than the benchmark model ( $P<0.01$ ). The above results further confirm the effectiveness of the PSO-BIM-Dematel causal network in controlling the accuracy of mechanical and electrical installation calculations.

## 5. Results & Discussion

To address the issue that accuracy control in mechanical and electrical installation heavily relied on manual experience, which caused large calculation errors, this study put forward an accuracy control model based on the PSO-BIM-Dematel causal network. The model extracted initial data, identified influencing factors through Dematel, and constructed a key factor matrix. PSO took the key factors determined by Dematel as variables and set quantity accuracy as the optimization target. It iteratively searched for the optimal solution through the PSO algorithm to determine the best parameter combination. The optimized parameters were then applied in BIM modeling to generate a visualized model. In the Datarade dataset test, the proposed model achieved a precision of 98.56%, which was 2%–5% higher than the comparison models, confirming its ability to accurately identify and measure various components. The recall reached 99.51% and the F1-score was 98.23%, both of which were significantly higher than those of the other models, demonstrating its dual advantages in both completeness and accuracy of quantity estimation. In classification tests across different mechanical and electrical types, the model achieved recognition rates of 0.99 for electrical systems, 0.99 for drainage systems, and 0.98 for mechanical systems. In contrast, the lowest recognition rates among the comparison models were only 0.93, 0.95, and 0.95, respectively. Compared to methods such as GIS-SEM or BIM-MICMAC that focus on static structural analysis, the superior performance of the PSO-BIM Dematel model proposed is due to its deep integration and complementarity of technical architecture. The dual iteration algorithm used by Bing YU et al. [14] in hydraulic engine optimization is effective in parameter optimization, but its optimization process is relatively closed and relies on accurate simulation models. The proposed model combines PSO with data-driven causal networks and has a stronger ability to explore optimal solutions in uncertain and high-dimensional BIM data.

In practical deployment, the proposed model can be integrated into existing BIM management platforms, using its visual interface to provide project managers with intuitive factor influence relationship networks and real-time calculation accuracy warnings, assisting in material procurement and schedule decision-making. However, the performance of the proposed PSO-BIM Demo model depends to some extent on the integrity and information granularity of the BIM model. If the initial model information is missing or the accuracy is insufficient, it may affect the accuracy of the final computational results. Therefore, future work will further focus on developing data augmentation algorithms with stronger robustness to BIM data, such as by introducing generative adversarial networks to

synthesize high-quality training data, or using pre-trained models to extract universal features to enhance the applicability of the model in scenarios with incomplete information.

## 6. Conclusions

In summary, the PSO-BIM-Dematel model combined Dematel's causal analysis with PSO's global optimization, performed causal relationship analysis and parameter optimization, and finally applied the results in BIM to realize visualized data and automated quantity estimation. The model showed strong adaptability and reliability in the refined identification and classification of complex mechanical and electrical systems, providing an advanced technical solution for quantity accuracy control in mechanical and electrical installation.

## References

- [1] Pan Y, Zhang L. Integrating BIM and AI for smart construction management: Current status and future directions. *Archives of Computational Methods in Engineering*, 2023, 30(2): 1081-1110.
- [2] Parekh R, Trabucco D. Recent progress in integrating BIM and LCA for sustainable construction: A Review. *International Journal of Science and Research Archive*, 2024, 13(1): 907-932.
- [3] Van Tam N, Quoc Toan N, Phong V V. Impact of BIM-related factors affecting construction project performance. *International Journal of Building Pathology and Adaptation*, 2023, 41(2): 454-475.
- [4] Al-Mohammad M S, Haron A T, Esa M. Factors affecting BIM implementation: Evidence from countries with different income levels. *Construction Innovation*, 2022, 23(3): 683-710.
- [5] Xiao Y, Bhola J. Design and optimization of prefabricated building system based on BIM technology. *International Journal of System Assurance Engineering and Management*, 2022, 13(Suppl 1): 111-120.
- [6] Saad A, Ajayi S O, Alaka H A. Trends in BIM-based plugins development for construction activities: a systematic review. *International Journal of Construction Management*, 2023, 23(16): 2756-2768.
- [7] Umar T. Challenges of BIM implementation in GCC construction industry. *Engineering, Construction and Architectural Management*, 2022, 29(3): 1139-1168.
- [8] Zhou D, Pei B, Li X, Jiang D, Wen L. Innovative BIM technology application in the construction management of highway. *Scientific reports*, 2024, 14(1): 1-16.
- [9] Chen Z, Chen L, Zhou X, Huang L, Sandanayake M, Yap P S. Recent technological advancements in BIM and LCA integration for sustainable

- construction: a review. *Sustainability*, 2024, 16(3): 1340-13040.
- [10] Zheng B, Hussain M, Yang Y, Chan A, Chi H. Trade-offs between accuracy and efficiency in BIM-LCA integration. *Engineering. Construction and Architectural Management*, 2025, 32(1): 237-258.
- [11] Banerjee T, Trivedi A, Sharma G M, et al. Analyzing organizational barriers towards building postpandemic supply chain resilience in Indian MSMEs: a grey-DEMATEL approach. *Benchmarking: An International Journal*, 2022, 30(6): 1966-1992.
- [12] Murugan M, Marisamynathan S. Analysis of barriers to adopt electric vehicles in India using fuzzy DEMATEL and Relative importance Index approaches. *Case studies on transport policy*, 2022, 10(2): 795-810.
- [13] Opanasenko V M, Fazilov S K, Mirzaev O N. An ensemble approach to face recognition in access control systems. *Journal of Mobile Multimedia*, 2024, 20(3): 749-768.
- [14] Bing Y U, Zhouyang L I, Hongwei K E. Wide-range model predictive control for aero-engine transient state. *Chinese Journal of Aeronautics*, 2022, 35(7): 246-260.
- [15] Wang Y, Fang S, Hu J. Active disturbance rejection control based on deep reinforcement learning of PMSM for more electric aircraft. *IEEE Transactions on Power Electronics*, 2022, 38(1): 406-416.
- [16] Fisher M M, Madolid J C, Demate E M. Assessing the Effectiveness of The PNP Internal Disciplinary Mechanism in Enhancing Job Satisfaction among Personnel. *International Journal of Multidisciplinary: Applied Business and Education Research*, 2025, 6(1): 431-452.
- [17] Eti S, Dinçer H, Yüksel S. Analysis of the suitability of the solar panels for hospitals: A new fuzzy decision-making model proposal with the T-spherical TOP-DEMATEL method. *Journal of Intelligent & Fuzzy Systems*, 2023, 44(3): 4613-4625.
- [18] Kao F C, Huang S C, Lo H W. A rough-fermatean DEMATEL approach for sustainable development evaluation for the manufacturing industry. *International journal of fuzzy systems*, 2022, 24(7): 3244-3264.
- [19] Gazi K H, Raisa N, Biswas A. Finding the most important criteria in women's empowerment for sports sector by pentagonal fuzzy DEMATEL methodology. *Spectrum of Decision Making and Applications*, 2025, 2(1): 28-52.
- [20] Gökalp Y, Eti S. Priority strategy development with intuitionistic fuzzy DEMATEL method for reducing energy costs in hospitals. *Journal of Soft Computing and Decision Analytics*, 2025, 3(1): 26-32.